Title	Dimensional Analysis of Thermoelectric Modules Under Constant Heat Flux
Author(s)	Suzuki, Ryosuke O.; Fujisaka, Takeyuki; Ito, Keita O.; Meng, Xiangning; Sui, Hong-Tao
Citation	Journal of electronic materials, 44(1), 348-355 https://doi.org/10.1007/s11664-014-3314-z
Issue Date	2014-08-05
Doc URL	http://hdl.handle.net/2115/59615
Rights	The final publication is available at link.springer.com
Type	article (author version)
File Information	Suzuki_ICT2013_Proc_4Rev2_NoMark.pdf

Instructions for use

Dimensional Analysis of Thermoelectric Modules under a Constant Heat Flux

Ryosuke O. Suzuki[1,2,*], Takeyuki Fujisaka[1,3], Keita O. Ito[1],

Xiangning Meng[1,4] and Hong-Tao Sui[1,5]

1. *Faculty of Engineering, Hokkaido University,*

2. *Japan Science and Technology Agency (JST), Core Research of Evolutional Science*

and Technology (CREST) researcher

3. Presently, *Nippon Steel & Sumitomo Metal Co. Ltd.*

4. *Japanese Society of Promotion of Science (JSPS) researcher* on leave from

Northeastern University, China

5. Presently, *Carl-Zeiss China*

* Corresponding author : Postal address: Kita-13Jou, Nishi-8Chome, Kita-ku, Sapporo, Hokkaido 060-

8628, Japan, Phone: +81 11 706 6339, Fax: +81 11 706 7882, e-mail: rsuzuki@eng.hokudai.ac.jp

Abstract

Thermoelectric power generation (TEG) is examined in case of the radiation heating. A constant heat flux is assumed in addition to the consideration of Seebeck effect, Peltier effect and Joule heat with the temperature dependencies of materials' properties. Numerical evaluations are conducted using combination of the finite-volume method (FVM) and an original simultaneous solver among the heat transfer, thermoelectric and electric transportation phenomena. The comparison with the experimental results shows that a new solver in numerical calculation could work well. The calculations predict that Seebeck effect becomes the larger because of the larger temperature difference when the thermoelectric (TE) elements are the longer. The heat transfer to the cold surface is critical to determine the junction temperatures under a constant heat flux from the hot surface. The negative contribution by Peltier cooling and heating can be minimized when the current is smaller at the longer elements. Therefore, the thicker TE module can generate the larger electric power even under a constant heat flux.   (163 words)

2

1   Introduction

Thermoelectric power generation (TEG) bases on the Seebeck effect and directly converts heat into electricity. Because TEG does not require a large-scale system, it has been studied as a method to recover unused heat [1], such as waste heat from automobiles [2], fuel cells [3] and marine engines [4], as well as solar heat [5,6]. Solar power generation using silicon photoelectric cells converts the solar energy at a wide range of wavelengths, but the energy from the longer waves in the infrared region is not used efficiently [7]. The residual energy is normally converted to heat, but this heat is not used as the effective energy resource. The energy density from the sun is too low to utilize the thermal heat directly as an electric power source, and the solar light concentrators such as convex and Fresnel lenses are indispensable [8]. A parabolic mirror is also effective to concentrate solar energy [9]. Our previous study proposed a water lens consisting of cheap materials such as a transparent sheet and natural water [10], where the cylindrical lens can obtain the two dimensional concentration such as a linear focus. The lens shape was optimized to achieve the maximum concentration ratio as high as 70 [11]. This value is not so high as the case of high performance plastic lens, but water lens can warm the thermoelectric (TE) surface mildly with the wider heating area.

The conversion efficiency in TEG systems is normally low when the temperature difference is low, and it becomes more effective to increase the hot-side temperature of TE module (TEM). The high concentration of solar energy onto the small surface of TEM is required to rise the temperature because the energy from the solar light is fixed by the receiving area of concentrator. When the convex lens concentrates the solar energy to a point focus, for example, only a single point in the TEM surface is heated and the other areas remain cold. Because the terminals of TE elements are spatially separated and normally covered by the ceramic insulator, the heat does not extend to the other terminals surrounding the hot spot. In order to heat the entire surface of TEM, the concentrated light should irradiate the whole TEM surface homogeneously. Its heating is desired to obtain the larger TE power so that the concentration ratio of the lens may be controlled [1]. Once a TE surface is heated by radiation, the heat transfer to another surface of TEM is steadily maintained to be constant. This irradiation heating of TEM is here considered for one of the TEG. Therefore, under a condition that a constant heat flows from the top surface of TEG system to the inside of module, we will consider how to maximize the TE power from TEM. In the conventional evaluations of TEG systems, many experimental studies were reported at the conditions that the surface temperatures were simply fixed at a certain value to maximize the TE performance [1]. However, this

constraint to keep the constant temperatures needs a lot of energy supply through a large

heat source, and it is indeed not realistic especially at the heat radiation. For example,

the mildly concentrated solar light warms the top surface of TEM and rises the surface

temperature. Therefore, its temperature is not fixed and the temperature difference at

two TE terminals depends on the irradiating heat flux and cooling capacity at the cold

surface.

Thermal radiation from the hot resources is also an attractive heat source because it

often appears in the industry. However, the detailed analysis of TEM was not studied.

TEG performance depends on the heat conduction from the thermal resources to the

cold terminals, and on the shape of TE modules as well as the material properties

(temperature dependencies of Seebeck coefficient, thermal conductivity and electrical

conductivity of TE elements, and thermal conductivities of insulators and electrode

materials). Therefore, it is necessary to analyze the system by combining the thermo-

mechanical aspect and electric circuit design.

The analytical approaches based on one-dimensional heat flow was reported in case

of constant heat flux [1,12,13], and it could express only the ideally approximated

conditions. However the heat fluxes to the two- or three-dimensional directions were

not considered because of the simplification for analytical solutions. It is required to

understand the construction of constant heat flow in the practical models in order to obtain the larger electrical power from the TEG.

The purpose of this work is to analyze the optimal dimensions of TE modules and their operating conditions in case of radiation heating. The material properties such as Seebeck coefficients, thermal and electrical conductivities are fixed as well as those of the other materials such as electrodes and insulators, and the suitable size of TE elements are considered to obtain the larger electrical power. A constant heat flux is assumed instead of a fixed temperature difference. When an external load is connected to this TEG, a current is introduced into a closed circuit. Once the current is introduced in a circuit, the Peltier heat cools at the hot terminals and it heats the cold terminals, respectively. Therefore, the contributions of Peltier effect and Joule heat in the TEM as well as Seebeck effect are important and their temperature dependencies as TE materials are required for precise analysis. However, because the temperature distribution is not homogeneous over the TE module, it is impossible to solve the simultaneous derivative equations in the analytical way as reported previously [12,13]. In this work the simultaneous derivative equations are numerically evaluated, based on the well-studied finite-volume method (FVM) and an original routine as the simultaneous solver among heat transfer and thermo-electric transportation phenomena [4,14-19]. This routine was

6

originally developed by Chen et al.[16,17] and implanted to our group. In order to investigate the effect of current, a new solver is coded by referring to Ref.16 and 17, and tried to apply this work. At present, the main effects of TEG can be also simulated by using the commercial optional software served from ANSYS, Inc., however, the contribution of Peltier heating and cooling due to the current generated by the Seebeck effect can not be analyzed. To visualize the effect of current during TEG, new routines for solver were coded.

2   Method

A brief outline of the procedures on the thermoelectric analysis is here described with our modifications [14]. Fundamental transport equations for heat can be expressed in derivative form as,

$$0 = \nabla \cdot (\kappa \nabla T) + \frac{1}{\sigma}|\boldsymbol{J}|^2 - T\boldsymbol{J} \cdot \nabla S \tag{1}$$

The first, second and third term in the right hand express the thermal diffusion, Joule heat, and Thomson effect, respectively. κ, σ, T, J, S are thermal conductivity, electronic conductivity, temperature, current density and Seebeck coefficient, respectively. From

the equation (1), the heat balance equations can be deduced in a simple case of one-dimensional model with the temperature-independent material parameters.

$$Q_h = K(T_h - T_c) + S_{pn}T_h I - 1/2 R I^2$$

$$Q_C = K(T_h - T_c) + S_{pn}T_C I + 1/2 R I^2$$

(2)

where Q_h, Q_c, K, T_h, T_c, S_{pn} and I are set as the heat at the hot inlet, that at the cold outlet, the total thermal conductance, temperatures at the hot and cold junctions, relative Seebeck coefficient and current in the circuit, respectively. S_{pn} is defined as S_p - S_n, where S_p and S_n are Seebeck coefficients intrinsic to p- and n-type materials, respectively. The equation (2) is often used as the one-dimensional thermal analysis. This study uses equation (1) for two- or three-dimensional analysis. The electric field can be written as,

$$\nabla \cdot (-\sigma \nabla V) = \nabla \cdot (S \sigma \nabla T)$$

(3)

where V is electric potential in the element. Therefore the current density is calculated from the temperature profile and potential distribution as,

$$\boldsymbol{J} = -S\sigma \nabla T - \sigma \nabla V$$

(4)

This $\boldsymbol{J}$ affects eq.(1) and then (3) thorough T. Therefore, the iteration of this calculation was performed >1000 times by using ANSYS software to obtain a stable and reproducible solution. The originally-coded function for TE evaluation is embedded in ANSYS Fluent (version 6) program, and the reproducible data were obtained after the

8

slow stabilization. This is because the contribution of current to the temperature profile

is weak, and the modification of current value is numerically delayed.

Fig.1 shows the characteristic layout of the TE elements used for the experiments and

simulation. *p*- and *n*-type elements are connected in series with copper electrode (0.3

mm thick). The upper and lower junctions are covered by alumina plate (0.8 mm thick).

The lower surface of alumina was kept at T_{CS} = 303 K, and the heat Q was

homogenously given from the top surface of the upper alumina plate. The TE module

consists of 71 pairs of TE elements. The size of the single element is 1.6x1.5x1.5 mm^3

both for *p*- and *n*-type elements. The open spacing among the elements is 1.0 mm. The

module size is 30mm x 30mm x 3.8mm.

Fig.2 shows the temperature dependencies of the Bi-Te elements in this commercial

module (European Thermodynamics, GM200-71-14-16). These data are used also for

numerical evaluation. Assuming the weakly concentrated solar light as reported

previously [10,11], Q was set to be 13.8 W for this module. This corresponds to the

energy density of 25900 W/m^2. The solar concentration ratio is set roughly 30 against

the natural solar light. This value was experimentally recorded as the typical

concentration ratio on a TEM surface when the cylindrical water lens consisting of

transparent sheet and water were used to focus in a single line [10,11]. In case of Frenel

lens this concentration ratio may arrive at 100 – 200, although the irradiated surface

area becomes as a point [1]. This paper assumes a mild and linear concentration such as

a case of the mild utilization of solar energy.

3　RESULTS AND DISCUSSION

3.1 Contact resistance

Several types of experimental setup were tested prior to the simulation, and compared

with the experimental data. Most of the calculated data were better than the

experimental data. An example is studied here to emphasis the effect of contact

resistance.

A lower surface of lower alumina plate in the TE module (Fig.1) is experimentally

kept at a constant temperature, while another surface is heated under a constant heat

flux in order to simulate the solar heat concentration.

Fig. 3 shows the temperature distribution calculated in two dimensional analyses.

Two-dimensional and steady heat flux from the hot part to the cold part is assumed, and

three-dimensional heat flow is not considered as the first approximation at this stage.

Because no strong heat flux to the three-dimensional directions exists in TEM as the

nature of structure, two-dimensionally analyzed data can be extended as the result in the three-dimensional model. The temperature dependencies of the materials were considered in the numerical calculation, but no strong dependencies of temperature on the position were found. The temperature distribution was smooth and continuous in two-dimensional space.

The temperature of the upper alumina plate decreases monotonically as the heat goes to the downstream. Due to Seebeck effect, the electric potential increases smoothly from the left side to the right side as shown in Fig. 3, and no clear temperature dependency of potential can be found in this scale. The current is defined as the current in the circuit when the external resistance is equivalent with the internal resistance. As shown in Fig.3, the distribution of current was not linear in the calculated conditions, and the maximum current density was found inside the metallic electrodes. Because the electrode is very thin, this high density is reasonable. However, it does not significantly decrease the circuit current because of the low electrical resistivity of these electrode materials. This numerical analysis could confirm the basic phenomena in the conventional analysis reported in the literatures, and it encourages us that our TE code in numerical calculation may be applied for the further analysis. It was important to check the workability and the practical applicability of our TE code.

Fig.4(a) and (b) shows the experimental distribution of temperature, voltage and power. Experimentally the adiabatic conditions were set toward the circumstances surrounding the TE module. A constant temperature at the cold surface was maintained by using the water-cooled copper plate and the TE module as a Peltier cooling device. Fig.4(b) showed a good coincidence in the voltage and power between the simulation and experimental data, if the contact resistance, r_C, is assumed. Because the internal resistance of TE module was measured as 1.092 Ω at room temperature, and r_C is evaluated as 0.126 Ω by subtracting the resistance of TE elements which was estimated from the measured cross-sectional area and length of TE elements. This r_C is as large as 10% of internal resistance, and it is enough large to affect the TE power as shown in Fig.4(b), although r_C is required to be minimized for the better performance of module.

In this case, the maximum output power, P_{max} = 0.217 W, was obtained at I = 0.311 A, and V = 0.697 V. From these data the total resistance in a circuit was calculated as 2.242 Ω. When we accept the criteria that the external resistance should be equal to the internal resistance to obtain P_{max}, the internal resistance is half of total resistance, i.e., 1.121 Ω. This value is very close to the experimental measurement (1.092 Ω), but slightly larger than it. It is reasonable because the electrical conductivity of TE material becomes lower at the higher temperatures, as shown in Fig.3(b).

As reported theoretically in the previous papers [14,20], however, the P_{max} would be obtained at the larger external resistance than the internal resistance if we consider both the effects of Seebeck and Peltier. When the resistance in the circuit is the larger, the voltage introduced by Seebeck effect will be consumed at the internal resistance, and the current induced into the circuit becomes the smaller. This current causes the Peltier effect at two electrodes and suppresses the temperature difference between two TE terminals, as shown in Fig.4(a). Because the Peltier heat becomes the smaller when the current is the smaller, the larger temperature difference can be obtained comparing with the case of the larger Peltier effect. In radiation heating the temperature difference between two terminals is determined by the balance of conductive heat and Peltier heat. Therefore, the temperature prediction by numerical analysis as shown in Fig.4(a) is useful. Fig. 4 thus confirmed the previous prediction by the authors [20], and as the current is quite sensitive to obtain P_{max}, the control of external resistance should be considered in the practical TEG using solar heat.

3.2 Cooling capacity

Fig.5 shows the calculated temperature distribution in the case shown in Fig.3. The surface temperature of lower alumina plate, T_{CS}, is inhomogeneous and wavy. The

simulation did not set a constant temperature, but a large heat transfer coefficient (1000 Wm^{-2}K^{-1}) was assumed. The thermal energy comes through the TEM, the roots of TE elements are heated by this thermal penetration, and the spacings among the elements are relatively well cooled. The surface temperature of upper alumina plate, T_{hs}, becomes more clearly wavy. Although the homogeneous heat radiation is given to the top surface, T_{hs} is not homogeneous but affected by the heat transfer toward the cooled area. The connecting positions with the TE elements are cooled even at the upper alumina plate. T_{hs} gradually decreases as a function of the distance. This can be understood as follows. The voltage generated by Seebeck effect due to a given temperature difference causes the current in the circuit, and its current forms Peltier effects that cools the hot terminal and heats the cooler terminal, respectively. As the junctions are connected in series, the current is common and the same degree of Peltier effect cools and heats the junctions. Then the temperatures, T_h and T_{hs}, decrease monotonically.

As shown in Fig. 5, the temperature drop at the alumina layer is only about 1.0 K, and the effective temperature difference, ΔT, between the junctions is about 46.5 K. Fig.6 shows the temperature difference between the junctions of p- and n-legs. When the heat transfer coefficient is set larger, namely the cold surface is cooled more strongly, the T_C can be lowered more effectively. However, the larger amount of heat is carried to the

14

colder part, and the hot junctions are also cooled the more strongly. Therefore, T_h

decreases at the higher heat transfer coefficient at the cold side, and ΔT becomes the

smaller. Oppositely when the heat transfer coefficient is set the smaller, T_C rises, and ΔT

becomes the smaller. Therefore, there exists a suitable heat transfer coefficient for

getting the larger ΔT, where an optimal heat balance is achieved between the cooling

effect of hot junctions and the heating effect of cold junctions. As shown in Fig. 6, h for

this optimal condition is close to 1000 $Wm^{-2}K^{-1}$, which is a little larger by air cooling

and is in a range of water cooling judging from the heat transfer in the normal

conditions. Therefore, in order that the radiation heating becomes more efficient, the

water cooling becomes necessary to generate electricity more effectively. The TEG

design is flexible depending on the environmental conditions as reported in many

literatures, however, from the view of efficient heat transfer, a strong cooling at the cold

surface is important to generate larger TE power, even at the heating by the constant

heat flux.

Fig.7 summarizes the dependency of maximum output power against the heat transfer

coefficient, h. The larger h may give a better power, but we may lose more energy to

obtain such a high h in the coolant.

3.3 Leg length

In order to get the larger ΔT under a constant heat flow, the longer leg length seems more effective because the thermal resistance becomes the larger. Fig. 8 shows the temperature distribution after the simulation when the leg length is varied in three levels. Temperature decreases smoothly and monotonically from the hotter area to the cool area in all three cases. The open circuit voltages in these modules shown in Fig. 8 are evaluated and shown in Fig. 9. The temperature profiles are also calculated when the external resistance is connected suitable to obtain the maximum output power. The open circuit voltage increases to the higher value as the leg becomes longer as shown in Fig. 9. When the current flows, however, the Peltier effect suppresses T_h due to the electric current.

The maximum output power, P_{max}, is evaluated as shown in Fig. 10. It increases as the module becomes thicker. Note that it decreases when the surface temperatures were set constant. The Joulic heat also affects to decrease P_{max}, although it contributes to increase T_h by the generated heat. Therefore, the decrease of T_h can be caused by Peltier cooling at the hot terminal, and it affects the non-linear increase in P_{max}.

4. CONCLUSIONS

A constant heat flow such as a solar light radiation heating is studied to design the thermoelectric (TE) power generation. Using the numerical evaluation based on the finite-volume method (FVM) and an original simultaneous solver among the heat transfer, thermoelectric and electric transportation phenomena, Peltier effect and Joulic heat with the temperature dependency of materials are evaluated. The numerical calculation offered a good simulation with the experimental behaviors, and it shows that the electrical contact resistance in the TE module causes an impedance shift that the optimal external resistance becomes larger than the internal resistance. Under a constant heat flux, the cooling capacity affects the temperature difference, and output power becomes better when h is greater than 1000 $\text{Wm}^{-2}\text{K}^{-1}$. The thicker TE module can give the larger output power although the Peltier cooling works to decrease the hot junction temperature.

REFERENCES

1. D.M. Rowe, "Thermoelectrics and Its Energy Harvesting, - Modules, Systems, and Applications in Thermoelectrics," vol.1 and 2, CRC Press, London, 2012.

2. D.M. Rowe, J. Smith, G. Thomas, G. Min, J. Electron. Mater. 40, 784 (2011).

3. X. Gao, S. J. Andreasen, M. Chen, S. K. Koer, International Jounal of Hydrogen Energy 33, 7137, (2008).

4. M. Chen, Y. Sasaki, R.O. Suzuki, Mater. Trans., 52, 1549 (2011).

5. N. Wang, L. Han, H, He, N. H. Park, K. Koumoto, Energy Environ. Sci. 4, 3676, (2011).

6. R. Singh, S. Tundee, A. Akbarzadeh, Solar Energy, 85, 371, (2011).

7. X. Ju, Z. Wang, G. Flamant, P. Li, W. Zhao, Solar Energy, 86, 1941, (2012).

8. W. T. Xie, Y. J. Dai, R. Z. Wang, K. Sumathy, Renewable and Sustainable Energy Reviews, 15, 2588, (2011).

9. Q.C. Murphree, Solar Energy, 70, 85, (2001).

10. R.O. Suzuki, A. Nakagawa, H.-T. Sui, and T. Fujisaka, J. Electron. Mater., 42 (7) 1960, (2013).

11. K. Ito, H. Sui, H.Hakozaki, H. Kinoshita and R.O. Suzuki, J. Electron. Mater., 43 (6), 2086-2093 (2014).

12. T. Kyono, R.O. Suzuki and K. Ono, IEEE Trans. On Energy Conversion, 18 (2), 330 (2003).

13. R.O. Suzuki and D. Tanaka, J. Power Sources, 122 (2) 201 (2003).

14. T. Fujisaka and R. O. Suzuki, Proc. IECON 2012 - 38th Annual Conference on IEEE Industrial Electronics Society, pp.5868-5872, (2012).

15. C. H. Cheng, S. Y. Huang, and T. C. Cheng, International Journal of Heat and Mass Transfer, 53, 2001, (2010).

16. M. Chen, L. A. Rosendahl, and T. Condra, International Journal of Heat and Mass Transfer, 54, 345, (2011).

17. M. Chen, S.J. Andreasen, L. A. Rosendahl, S.K.Kaer amd T. J. Condra, J. Electron. Mater., 39, 1593, (2010).

18. J. Xiao, T. Yang, P. Li, P. Zhai, and Q. Zhang, Applied Energy 93, 33, (2012).

19. X. R. Palacios, A. Arenas, R. R. Pecharromán, and F.L. Pagola, Applied Thermal Engineering, 29, 3501, (2009).

20. T. Fujisaka, H-T.Sui and R.O. Suzuki, J. Electron. Mater., 42, 1688, (2013).
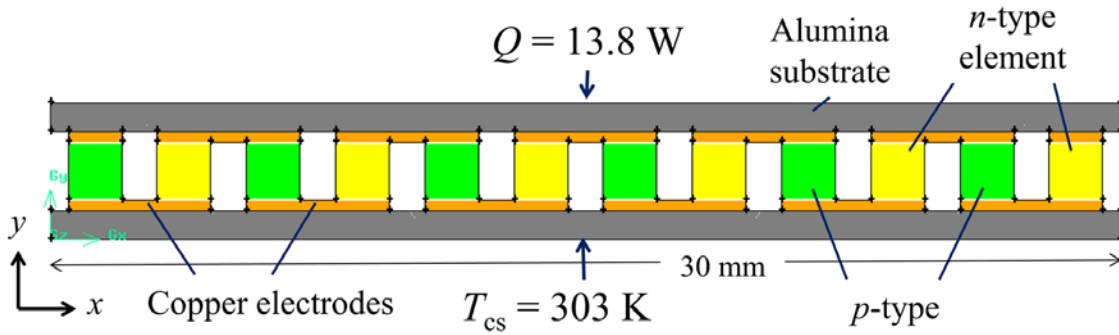
Figure Captions

Fig. 1 A model analyzed. A constant heat flow of 13.8 W is introduced to the TE

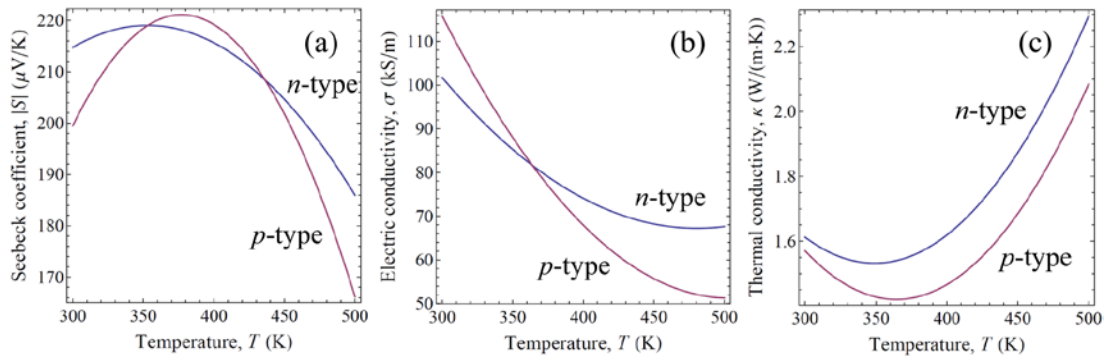module whose cold surface is kept at 303 K.

Fig. 2 Temperature dependencies of the studied Bi-Te elements. (a) Seebeck coefficient,

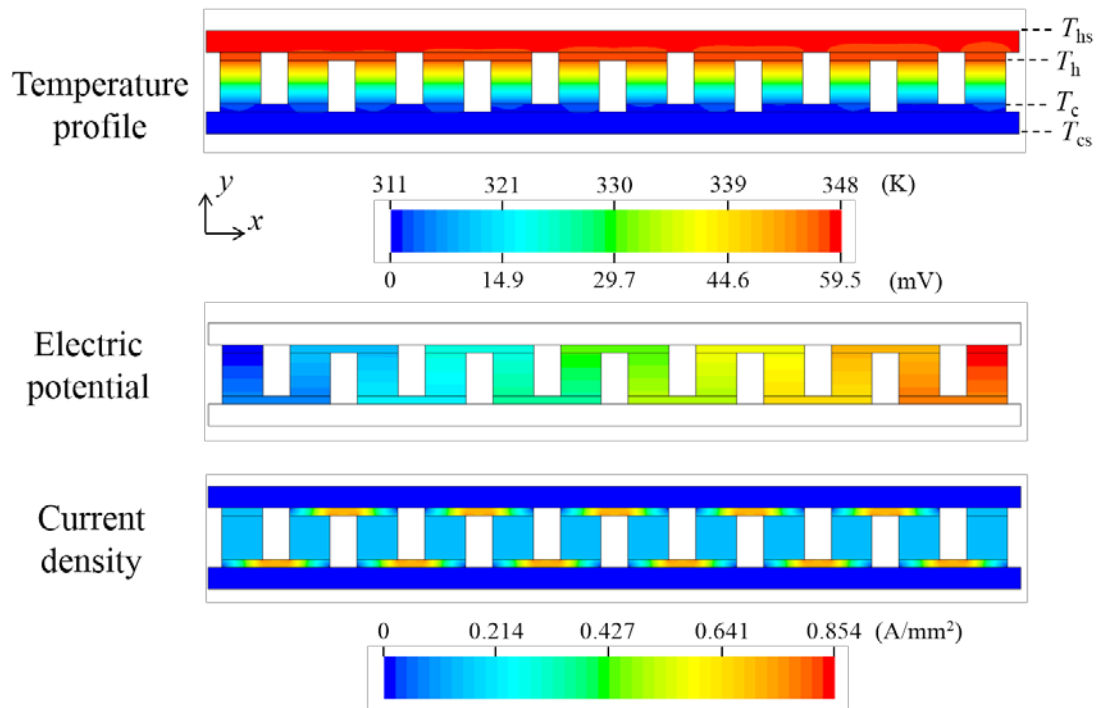(b) electric conductivity and (c) thermal conductivity.

Fig. 3 Distribution of temperature, electric potential and current density after simulation.

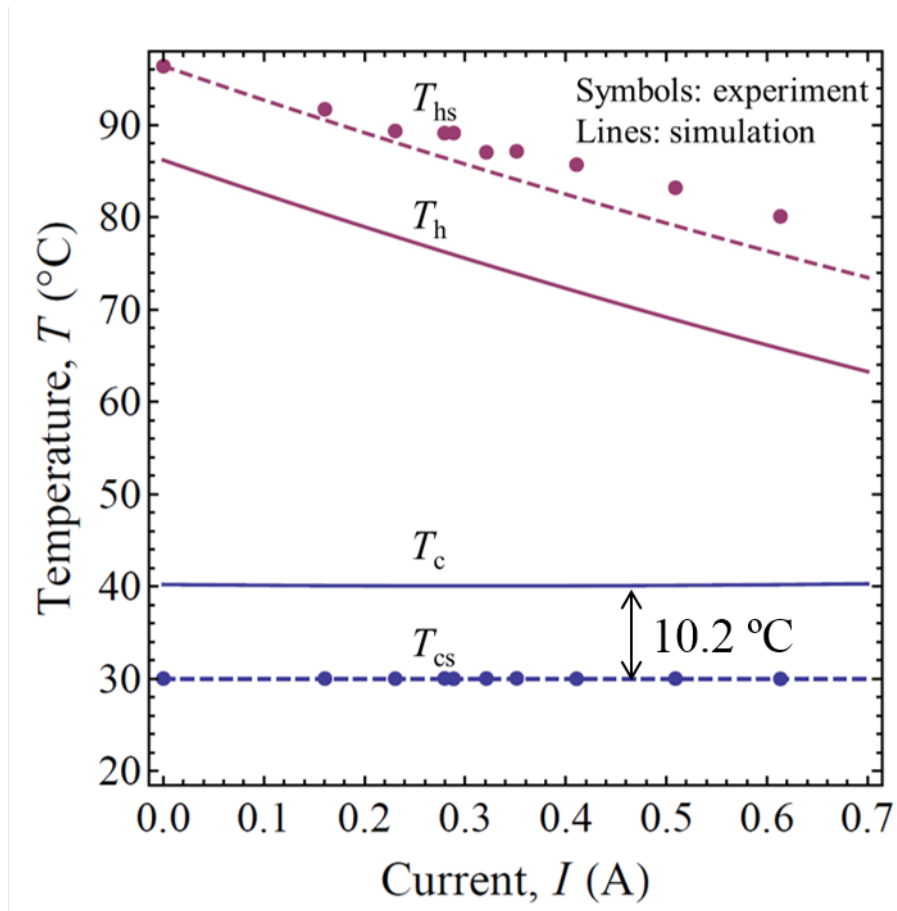Color bars indicate the measure of the counter plots.

Fig. 4 (a) Temperatures at the alumina surface, where T_C, T_{CS}, T_{hs}, and T_h are the

temperatures at the upper and lower surface of the lower alumina plate, and those at the

upper and lower surface of the upper alumina plate, respectively. (b) Voltage and
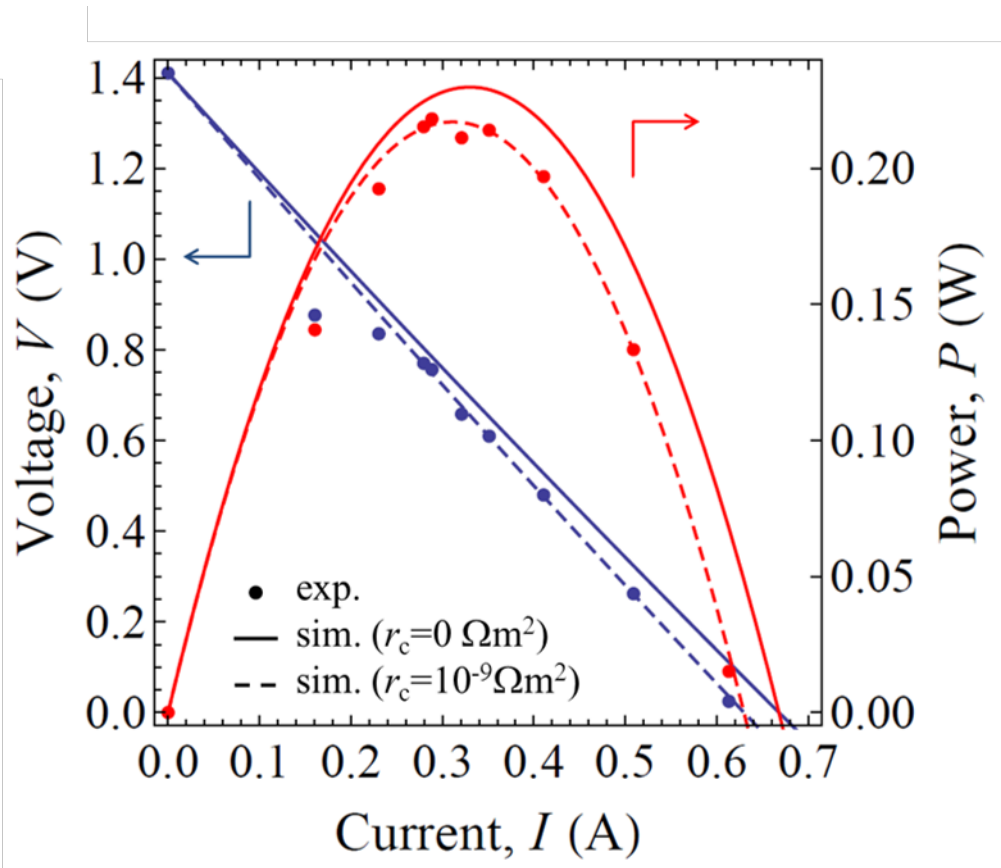
powder obtained in the experiments and simulations at two contact resistance, r_C.
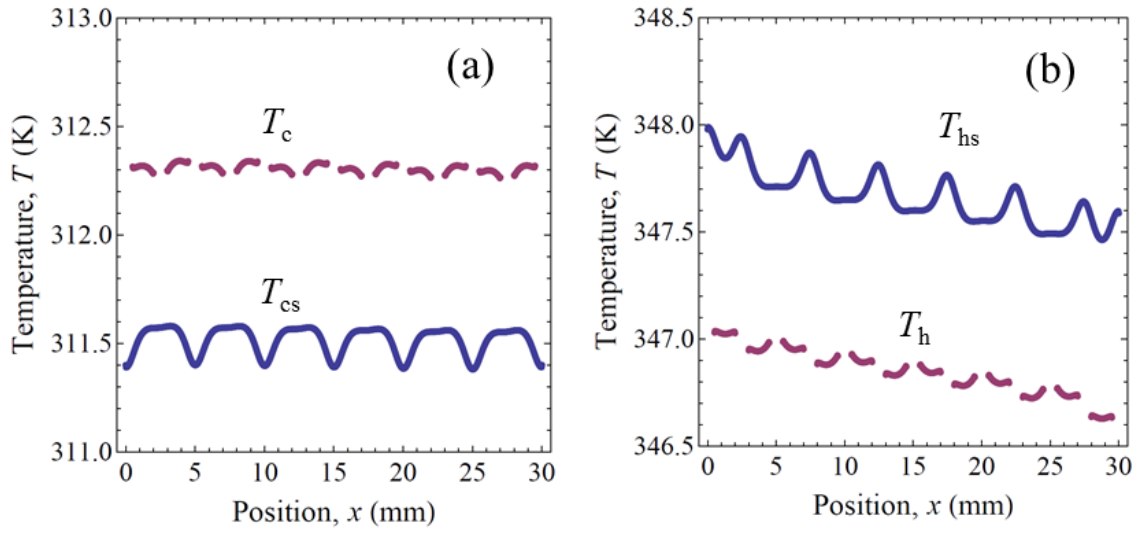
Fig. 5 Simulated temperatures (a) at the lower alumina plate and (b) at the upper

alumina plate.

Fig.6 Temperature difference between the junctions of p- and n-legs. T_h and T_c are

junction temperatures.

Fig.7 Maximum power depending on the heat transfer coefficient at the colder side.

Fig.8 Temperature distribution in TE module. The leg length is (a) 1.6 mm, (b) 3.2 mm and (c) 4.8 mm.

Fig.9 Leg length dependency of junction temperatures, T_h and T_c, when the optimal external resistance is connected.

Fig.10 Dependency of maximum power, P_{max}, on leg length, d, when the optimal external resistances are connected.

Fig.1 A model analyzed. A constant heat flow of 13.8 W is introduced

to the TE module whose cold surface is kept at 303 K.

Fig.2 Temperature dependencies of the studied Bi-Te elements.

(a) Seebeck coefficient, (b) electric conductivity and (c) thermal conductivity.

Fig. 3 Distribution of temperature, electric potential and current density after simulation. Color bars indicate the measure of the counter plots.

Fig.4 (a) Temperatures at the alumina surface, where T_C, T_{CS}, T_{hs}, and T_h are the temperatures at the upper and lower surface of the lower alumina plate, and those at the upper and lower surface of the upper alumina plate, respectively.

Fig. 4 (b) Voltage and power obtained in the experiments and simulations

at two contact resistance, r_C.

Fig.5 Simulated temperatures

(a) at the lower alumina plate and (b) at the upper alumina plate.

Fig.6 Temperature difference between the junctions of *p*- and *n*-legs.
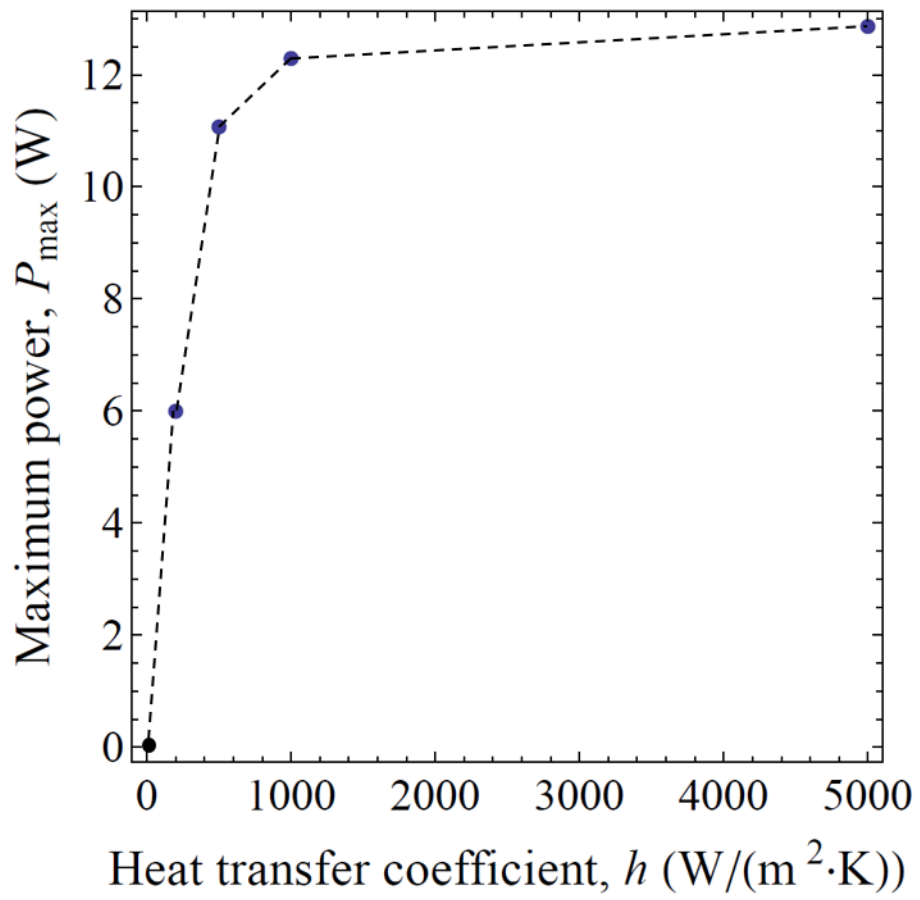
T_h and T_c are junction temperatures.

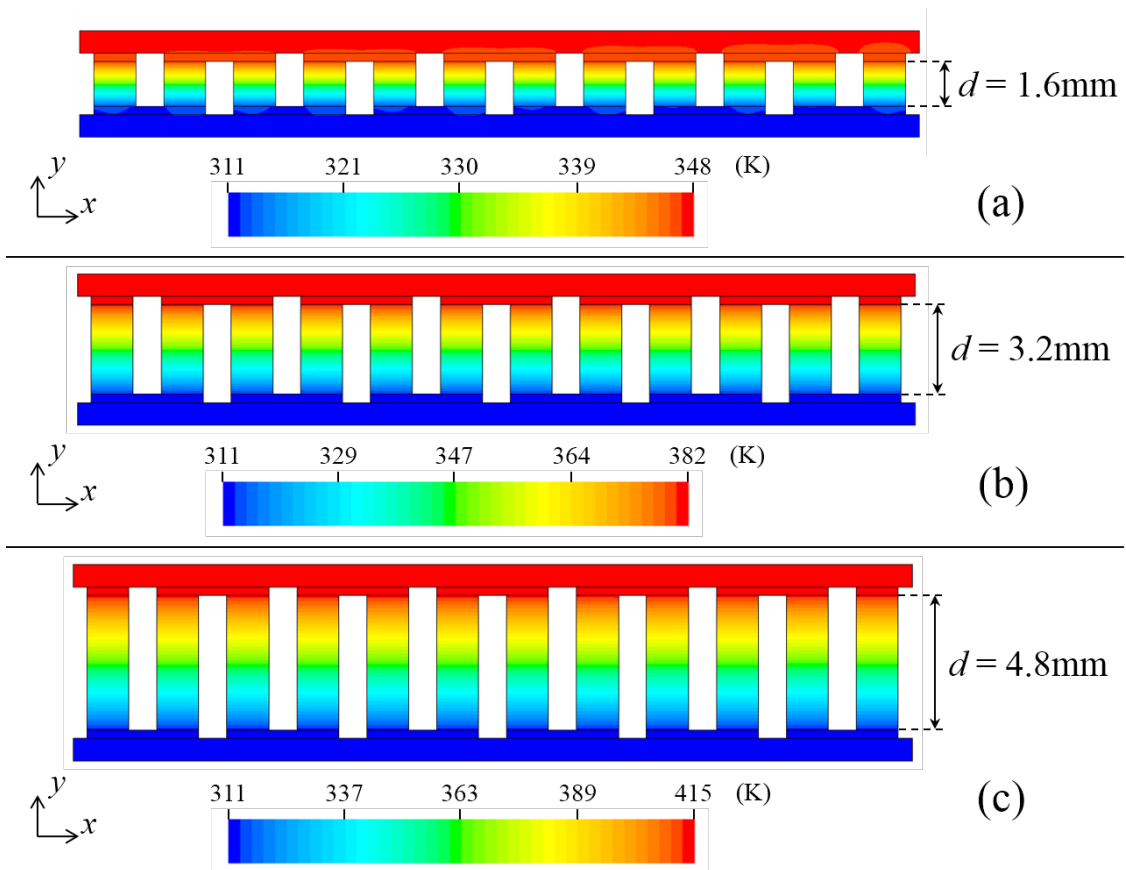**Fig.7** Maximum power depending on the heat transfer coefficient at the colder side.

Fig.8 Temperature distribution in TE module.

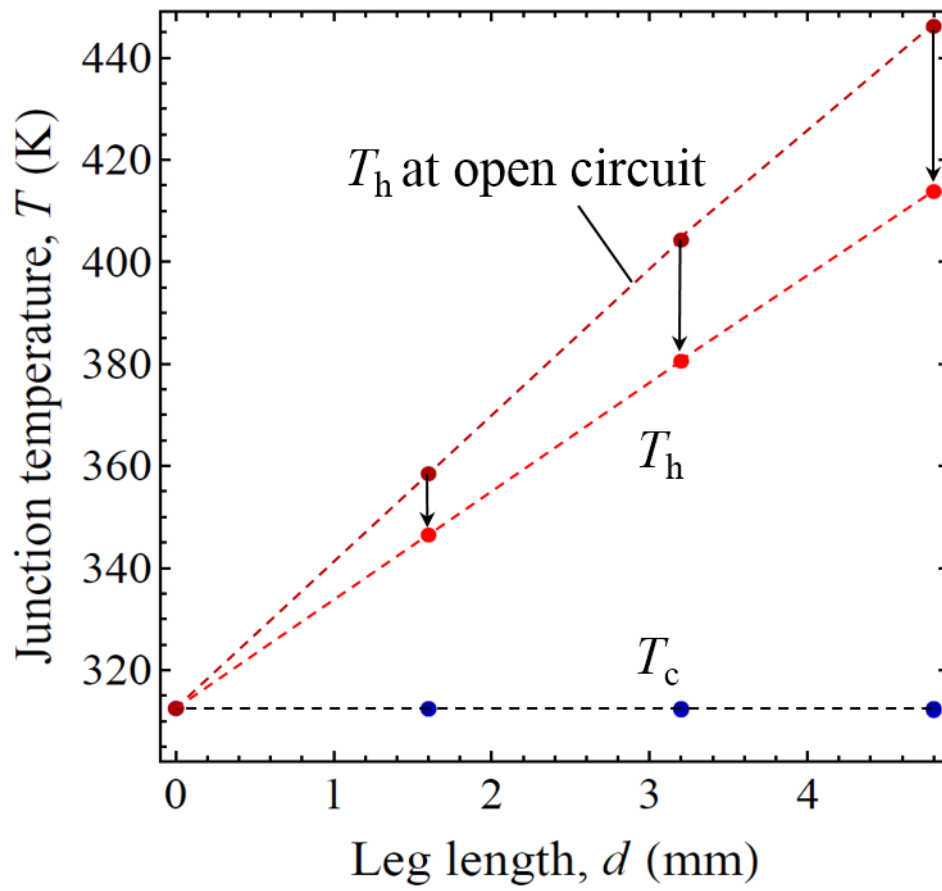The leg length is (a) 1.6 mm, (b) 3.2 mm and (c) 4.8 mm.

Fig.9 Leg length dependency of junction temperatures, T_h and T_c,

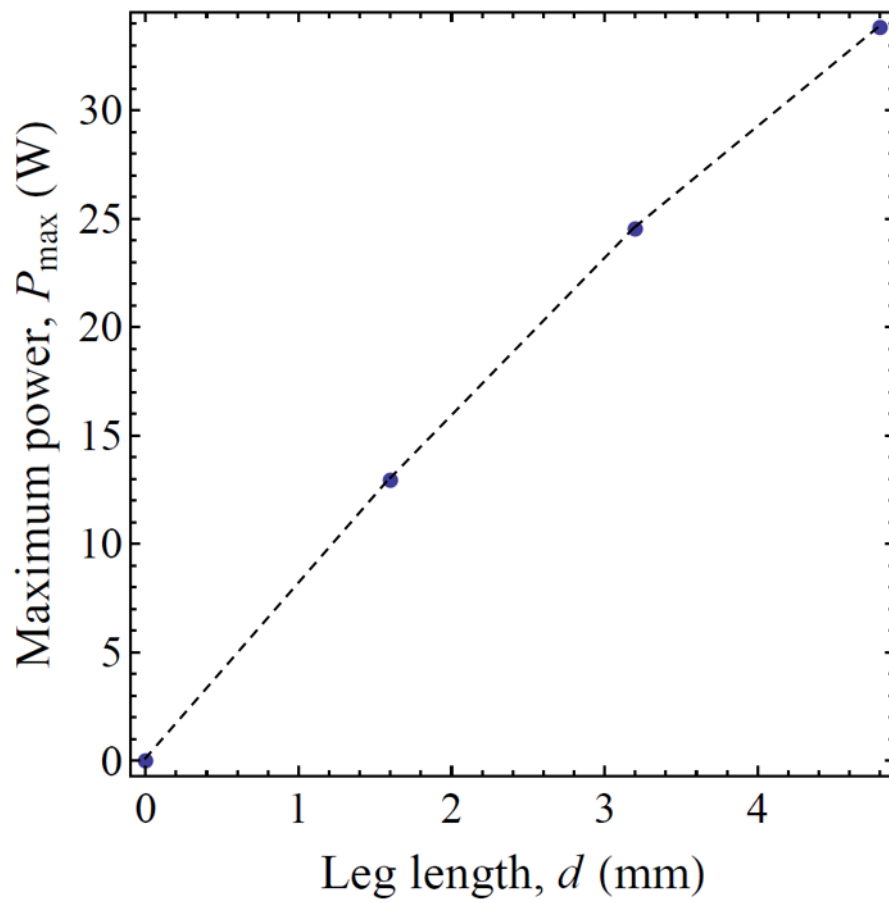when the optimal external resistance is connected.

Fig. 10 Dependency of maximum power, P_{max}, on leg length, d, when the optimal external resistances are connected.